



## Sorption of HDTMA cations on Croatian natural mordenite tuff

Mirela Rožić<sup>a,\*</sup>, Snežana Miljanić<sup>b</sup>

<sup>a</sup> University of Zagreb, Faculty of Graphic Arts, Getaldićeva 2, 10000 Zagreb, Croatia

<sup>b</sup> University of Zagreb, Faculty of Science, Department of Chemistry, Laboratory of Analytical Chemistry, Horvatovac 102a, 10000 Zagreb, Croatia

### ARTICLE INFO

#### Article history:

Received 11 February 2010

Received in revised form

15 September 2010

Accepted 15 September 2010

Available online 22 September 2010

#### Keywords:

Mordenite tuff

Hexadecyltrimethylammonium Cation

Sorption

### ABSTRACT

Sorption of the cationic surfactant, hexadecyltrimethylammonium cations (HDTMA), on the solid/liquid interface of the natural mordenite tuff (MT) was studied. The examined tuff originated from Croatia consisting of 30% of mordenite. SEM observations confirmed the crystalline nature of mordenite which can be described in terms of aggregates of many small platelets with diameters in the range of 1  $\mu\text{m}$ . Studying the porosity properties of MT, it was found that the average pore diameter (4.42 nm) between mordenite's platelets allows penetration of HDTMA cations. The measurements of zeta potential indicated that in MT samples with surfactant concentration in the range between 0.013 and 0.25 mmol/g, HDTMA cations fill the mesopores of MT. By further increase in HDTMA concentration, the surfactant sorbs on the external zeolite surface, as revealed by the SEM micrographs. Vibrational (FTIR and FT Raman) spectra showed that in the MT samples with initial HDTMA concentration from 0.013 to 0.25 mmol/g, alkyl chains adopt mainly *gauche* conformation, whereas in the MT samples with higher initial HDTMA concentrations *trans* conformers are predominant and form a highly ordered structure on the mordenite surface.

© 2010 Elsevier B.V. All rights reserved.

### 1. Introduction

Zeolites are highly crystalline aluminosilicates, described by the general formula  $M^{n+}_{x/n}[(\text{AlO}_2)_x(\text{SiO}_2)_y]^{x-} \cdot z\text{H}_2\text{O}$  (where M is a metal cation, a proton or, less frequently, a charged molecule) and having as characteristic feature a three-dimensional, regular array of intracrystalline nanovoids. In the process of formation of synthetic or natural zeolites, by substituting the Si atoms by Al atoms, a net formal charge (−1) is created at the Al–O tetrahedra which must be balanced by a positive counterion in order to ensure electrical neutrality [1]. Due to ability to attract positively charged ions, zeolites are widely used for sequestration of cations, particularly the relatively small ones such as ammonium and metal ions [2–7].

Surfactant adsorption and intercalation has been the subject of numerous studies involving clay minerals [8–17] and synthetic zeolites [2,18–20]. While extensive research has been done on sorption of surfactants on the natural zeolite clinoptilolite tuffs [21–28], only a few studies aimed at modification of the natural mordenite tuffs [29].

Surfactant modified zeolites and clay minerals have been developed by treatment with surface modifiers such as hexadecyltrimethylammonium bromide and tetramethylammonium bromide [2]. These modified minerals are particularly attractive since they can sorb organic compounds, inorganic cations and inor-

ganic anions. The positively charge head groups are balanced by anionic counterions making surfactant modified zeolites and clays potential sorptive media for anionic contaminants. Oxyanions such as arsenate can be sorbed from water onto the alternated mineral surface via an ion exchange mechanism [12,20,22,25,26,30]. On the other hand, phenol, benzene, xylene, pyrene, naphthalene can be sorbed on organozeolites and organoclays owing to the increased hydrophobicity of the mineral surface after replacement of hydrated cations with various organocations [8,9,12,25,28,31]. The sorption of hydrophobic organic contaminants seems to be due to partitioning of organics into the organic pseudo phase created by the surfactant tail groups [12,25,27,28].

The aim of the present work was to study the sorption phenomena of hexadecyltrimethylammonium cations on the natural mordenite tuff (MT). Sorption of HDTMA cations on MT was studied and zeta potentials of modified MT samples were determined. Based on the textural properties of the MT, FT infrared and Raman spectra of the MT samples as well as on the SEM micrographs of the original and modified zeolite surface, a mechanism of HDTMA sorption on MT was proposed.

### 2. Experimental

#### 2.1. Materials

Quaternary ammonium salt hexadecyltrimethylammonium bromide, (HDTMABr, Merck), with a molar mass of 364.46 g/mol and a minimum of 99% of active substance was used. Critical micelle

\* Corresponding author. Tel.: +385 1 23 71 080; fax: +385 1 23 71 077.

E-mail addresses: [mirela.rozic@grf.hr](mailto:mirela.rozic@grf.hr), [mirelarozic@yahoo.co.uk](mailto:mirelarozic@yahoo.co.uk) (M. Rožić).

concentration (CMC) of HDTMABr at 30 °C was 0.94 mmol/dm<sup>3</sup>, as estimated by conductivity measurements of aqueous HDTMABr solutions of different concentrations.

Sorption of HDTMA cations was applied to a mordenite tuff from Croatia (Cerje Jesenjisko, Hrvatsko zagorje). Particles of the MT samples were smaller than 0.125 mm. The mineralogical composition of MT was determined by X-ray powder diffraction (XRD) using a Philips diffractometer PW 1830 with Cu K $\alpha$  radiation. Data were collected between 5° and 60° 2 $\theta$  in a step scan mode with steps of 0.02° and counting time of 5 s. The chemical composition of MT was determined by classical chemical analysis. The cation exchange capacity (CEC) of MT was determined by measurement of equilibrium concentrations of exchangeable cations (Na<sup>+</sup>, K<sup>+</sup>, Ca<sup>2+</sup> and Mg<sup>2+</sup>) in the supernatant by atomic absorption spectrometry (AA-6800, Shimadzu) after saturation of the samples with NH<sub>4</sub><sup>+</sup> ions [32].

## 2.2. Methods

### 2.2.1. Sorption of HDTMA cations onto MT samples

Surfactant solutions were prepared with deionised water. Concentrations of HDTMA cations were from 0.045 to 55 mmol/dm<sup>3</sup>. Mixtures of 2.0 g of MT and 0.1 dm<sup>3</sup> of surfactant solutions were stirred at 30 °C (above Krafft point which is 25 °C) during 48 h on a mechanical shaker (Innova 4080) at 150 rpm. Krafft point is the temperature above which solubility of the surfactant rises sharply. At this temperature a phase change of the surfactant occurs, turning a clear surfactant solution into a turbid one. Duration of stirring (48 h) has been chosen due to comparison with the sorption of the HDTMA cations on clinoptilolite tuffs studied in our previous work [24]. Thereafter 0.05 dm<sup>3</sup> of each mixture was centrifuged (3000 rpm for 5 min) and a supernatant was analyzed. The concentration of a residual surfactant cation was determined as a content of the total organic carbon in the obtained supernatants (Shimadzu TOC-5050A analyzer). Concentration of the sorbed HDTMA cation in mmol/g was calculated using the mass balance equation:

$$Q_e = (c_0 - c_e) \frac{V}{m} \quad (1)$$

where  $c_0$  and  $c_e$  are the initial and equilibrium liquid-phase concentrations of the surfactant cation (mmol/dm<sup>3</sup>), respectively;  $V$  is the volume of the surfactant solution (dm<sup>3</sup>), and  $m$  is the mass of the mordenite tuff sample (g).

The surfactant modified samples were filtered through the filter paper (blue band) on the Büchner funnel. The samples were washed with distilled water until a reaction with 1% AgNO<sub>3</sub> solution was negative. The modified samples were dried at the room temperature.

### 2.2.2. Determination of the permanent surface charge

The permanent charge resulting from isomorphous substitution of silicium by aluminium in the crystal structure of mordenite was determined by potentiometric titration with HCl,  $c = 0.01$  mol/dm<sup>3</sup> [33]. 0.5 g of MT and 0.025 dm<sup>3</sup> of demineralised water were stirred until the pH stabilized. Then aliquots of 0.02 cm<sup>3</sup> of HCl solution were added to the prepared mixture, and the pH, when became constant, was recorded. The permanent surface charge,  $\sigma_H$ , was calculated by subtracting the net consumed amount of protons in the supernatant,  $n_H^{\text{sup}}$ , from the net consumed amount of protons in the suspension,  $n_H^{\text{susp}}$ , according to the equation:

$$\sigma_H = \frac{1}{m} (n_H^{\text{susp}} - n_H^{\text{sup}}) \quad (2)$$

where  $m$  is the mass of the sample (g), and  $n$  is the amount, indicated in mmol. The permanent surface charge of the MT was taken as the external cation exchange capacity (ECEC) of the mordenite tuff.

### 2.2.3. Determination of textural properties

The specific surface area, the cumulative pore volume and the average pore diameter of MT samples were determined using Brunauer–Emmet–Teller (BET) N<sub>2</sub> gas adsorption–desorption isotherms measured at 77 K on a Micromeritics ASAP-2000. The samples were previously degassed at 473 K for several hours under medium vacuum of 0.67 Pa.

### 2.2.4. Electrokinetic (zeta) potential measurements

The zeta potential of MT samples was measured by a Zetasizer 3000 instrument. The electrophoretic mobility of the particles was automatically calculated and converted to the zeta potential using the Smoluchowski equation. Each MT sample (0.010 g) was suspended in redistilled water (0.050 dm<sup>3</sup>) by mixing for 15 min. The samples were allowed to stand for 5 min. An aliquot taken from the supernatant was used for measurements of zeta potential. The average value of 10 measurements was taken as a representative potential.

### 2.2.5. Scanning electron microscopy

An energy dispersive X-Ray spectrometer (SEM-EDS), “TESCAN VEGA TS5136LS” with the EDS detector microscope was used for taking the SEM micrographs of the natural and modified MT surface. Specimens for SEM observations were prepared by coating the MT powder with a thin gold/palladium layer by SC7620 Sputter Coater Quorum.

### 2.2.6. FT infrared spectroscopy

FTIR spectra were taken on a Bruker Equinox 55 interferometer using the KBr pressed disk technique. For each KBr pellet, 1 mg of tuff and 100 mg of KBr were weighted, grounded in an agate mortar, and pressed. Spectra were recorded over the spectral range between 4000 and 400 cm<sup>-1</sup> with a resolution of 4 cm<sup>-1</sup>.

### 2.2.7. FT Raman spectroscopy

FT Raman spectra were measured on a Bruker Equinox 55 interferometer equipped with a FRA 106/S Raman module using Nd-YAG laser excitation at 1064 nm and the laser power of 500 mW. Spectra were taken in the 100–3500 cm<sup>-1</sup> range. To obtain a good spectral definition, 1000 scans at a spectral resolution of 4 cm<sup>-1</sup> were averaged for each sample.

## 3. Results and discussion

### 3.1. Mineralogical and chemical analysis

The mineral content of MT, based on XRD analysis was 30% of mordenite, 30% of K-feldspars and 40% of low quartz (Fig. 1). In powder XRD patterns no significant differences were observed between the original MT sample and the samples of HDTMA modified MT, showing that the crystalline structure of mordenite remained unchanged during these modifications.

Results of the quantitative chemical composition of the studied MT are given in Table 1.

### 3.2. Cation exchange capacity (CEC)

Results of the CEC determination showed that the main exchangeable cations in the sample of MT were Ca<sup>2+</sup> and Na<sup>+</sup> ions (Table 2). The natural MT had CEC of 0.915 mequiv./g.

### 3.3. The surface charge

Coverage of sorbed protons on the surface of the MT,  $\sigma_H$ , was calculated using Eq. (2). A maximal value of 0.105 mmol/g was

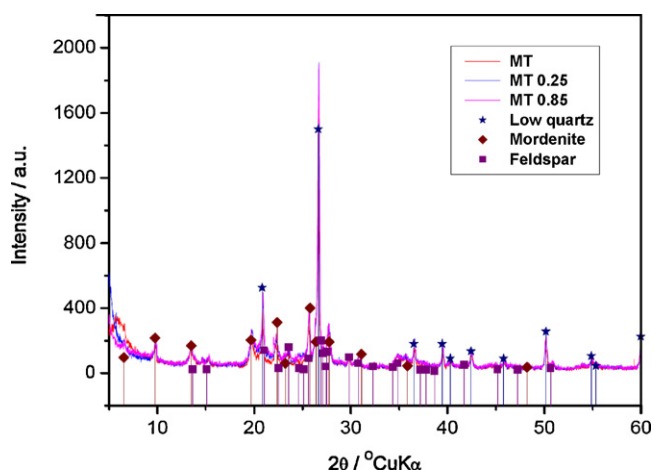


**Fig. 1.** X-ray powder patterns of the original MT sample (MT) and the MT samples with initial concentration of HDTMA cations 0.25 mmol/g (MT 0.25) and 0.85 mmol/g (MT 0.85).

**Table 1**  
Chemical analysis of the mordenite tuff.

	Weight/%
SiO <sub>2</sub>	70.44
TiO <sub>2</sub>	0.19
Al <sub>2</sub> O <sub>3</sub>	11.34
Fe <sub>2</sub> O <sub>3</sub>	1.04
FeO	0.13
MnO	0.02
MgO	0.20
CaO	1.75
Na <sub>2</sub> O	0.94
K <sub>2</sub> O	1.97
Loss by glowing at 1000 °C	11.80

obtained at pH 2.5 (Fig. 2). This value was considered as the value of the external CEC of the mordenite tuff.

### 3.4. Sorption of HDTMA cations

Sorption of HDTMA cations on the MT sample is presented in Fig. 3. A maximum value of the sorbed HDTMA cations on MT was achieved in solutions of initial HDTMA concentrations higher than 35 mmol/dm<sup>3</sup>. Thus, in solutions of 35 and 55 mmol/dm<sup>3</sup>, HDTMA was sorbed on MT in amount of 0.88 and 0.90 mmol/g, respectively. Obtained values were almost four times higher than those for clinoptilolite tuffs reported in our previous work [24], which had been between 0.160 and 0.250 mmol HDTMA/g. It was showed for clinoptilolite tuffs that reaction in the system of clinoptilolite and HDTMA cations involves only external cation exchange capacity (ECEC, fraction of total CEC), leaving the internal CEC unchanged [12]. As can be seen a quantity of the sorbed HDTMA cations on the MT is equal to the CEC of the MT.

### 3.5. Textural properties of MT samples

The specific surface area and porosity properties of the natural MT and the MT samples with 0.25 and 0.85 mmol/g sorbed

**Table 2**  
Cation exchange capacity of the mordenite tuff.

Sample	Exchanged cations/mequiv./g			
	Na <sup>+</sup>	K <sup>+</sup>	Mg <sup>2+</sup>	Ca <sup>2+</sup>
Mordenite tuff	0.384	0.062	0.077	0.392

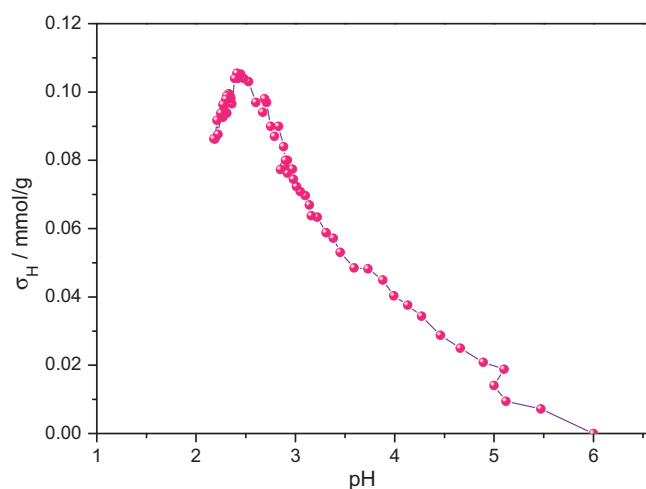


**Fig. 2.** A plot of pH vs surface charge of mordenite tuff.

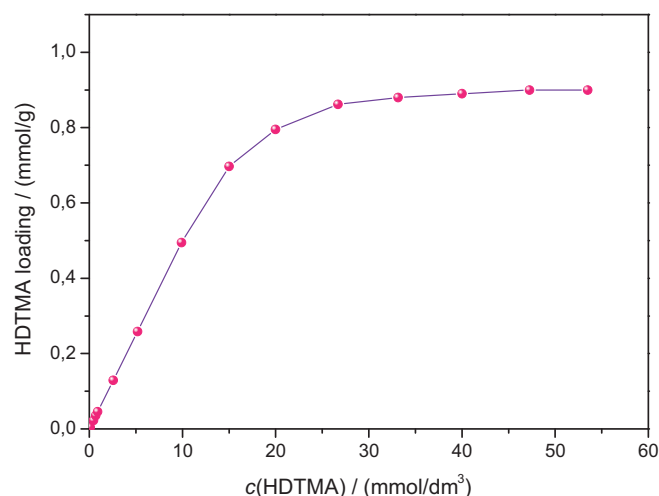


**Fig. 3.** Sorption of HDTMA cations onto mordenite tuff after 48 h stirring.  $c(\text{HDTMA})$  is the initial concentration of HDTMA cations in solution.

HDTMA are given in Table 3. In case of the unmodified MT, the specific surface area was 42.11 m<sup>2</sup>/g, the cumulative pore volume was  $5.79 \times 10^{-2}$  cm<sup>3</sup>/g and the average pore diameter was 4.42 nm. For the MT sample containing 0.25 mmol HDTMA/g significantly smaller specific surface area and cumulative pore volume were measured, 6.19 m<sup>2</sup>/g and  $3.36 \times 10^{-2}$  cm<sup>3</sup>/g, respectively, while the average pore diameter was larger ( $d = 18.96$  nm), when compared to the natural MT. A higher loading of HDTMA cations on the MT (0.85 mmol/g) resulted only in a slight variation of the obtained values with respect to the MT sample with 0.25 mmol HDTMA/g (Table 3).

The average pore diameter of the original MT (4.42 nm) is larger than the length of the HDTMA alkyl chain, 2.3 nm, thus allowing penetration of organocations into these pores [34]. It can be assumed that HDTMA cations sorb in the narrow mesopores placed

**Table 3**  
The specific surface area, the cumulative pore volume and the average pore diameter of the MT samples. Labels 0.25 and 0.85 denote initial amounts (mmol/g) of sorbed HDTMA cations.

Sample	$S_{\text{BET}}/\text{m}^2/\text{g}$	$V/\text{cm}^3/\text{g}$	$d/\text{nm}$
MT	42.11	$5.79 \times 10^{-2}$	4.42
MT 0.25	6.19	$3.36 \times 10^{-2}$	18.96
MT 0.85	4.74	$2.50 \times 10^{-2}$	18.26

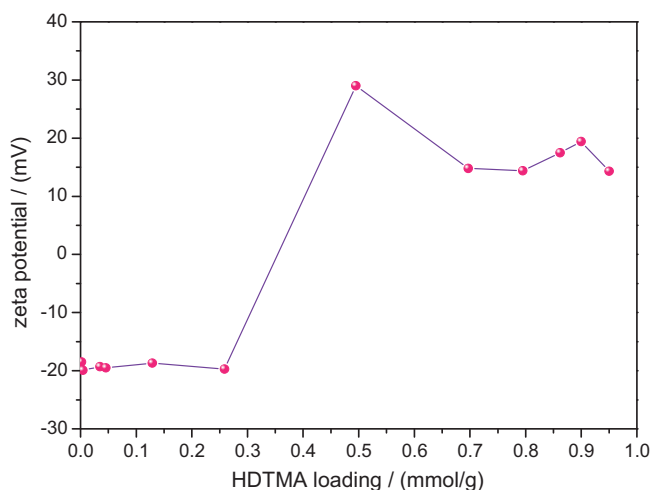


Fig. 4. Zeta potential of the mordenite samples vs HDTMA loading.

between mordenite crystals in the tuff. A decrease in the surface area and the pore volume was due to obstruction of mesopores by HDTMA cations, thus impeding the diffusion of  $N_2$  throughout these channels.

### 3.6. Electrokinetic (zeta) potentials

The results of determination of zeta potentials of the natural and surfactant modified MT samples are presented in Fig. 4. The measurements of zeta potential revealed that the surface of the examined MT sample acquires a negative charge ( $-20$  mV) in water at natural pH.

An isoelectric point (IEP) is characterized by the value zero for electrokinetic potential. Under these conditions, negative MT surface charges are neutralized. At the IEP of the surfactant modified MT sample, HDTMA concentration was approximately  $8 \text{ mmol dm}^{-3}$ . An adequate load of HDTMA cations was  $0.35 \text{ mmol/g}$  (Fig. 4), which was more than the external CEC of MT ( $0.105 \text{ mmol/g}$ ). For comparison, at the IEP, clinoptilolite had been loaded at its external CEC resulting in a monolayer coverage [31]. Therefore it might be concluded that at the zero potential, HDTMA cations are not only immobilized on the external surface of mordenite but situated in the mesopores, too.

This was also confirmed by the values of zeta potential which did not vary for HDTMA loadings less than  $0.25 \text{ mmol/g}$ . Since a zeta potential is a measure of a potential of an external surface, it can be assumed that HDTMA cations in an amount up to  $0.25 \text{ mmol/g}$  penetrated in narrow mesopores of mordenite. Further sorption in an amount of the ECEC ( $0.105 \text{ mmol/g}$ ) was attributed to the sorption of the HDTMA cations on the external surface of the mordenite crystals. At the total HDTMA loading of  $0.35 \text{ mmol/g}$ , external monolayer coverage of HDTMA was formed, making the MT surface hydrophobic.

The highest zeta potential was obtained for the MT sample with  $0.50 \text{ mmol HDTMA/g}$  and assigned to formation of a bilayer on the external surface of the mordenite crystals. By further increase of the HDTMA loadings zeta potentials slightly decreased, most likely due to sorption of the surfactant micelles in larger mesopores of the tuff and their leaching during the treatment of modified samples in distilled water.

### 3.7. Scanning electron microscopy

The size and shape of zeolite crystals are of paramount importance for their performance in any particular application. The

change in crystal size and morphology alters the performance in terms of apparent activity, selectivity, ion exchange capacity and the rate of adsorption by influencing the characteristic diffusion through the crystallites [35].

Scanning electron micrographs of the original mordenite tuff and those with  $0.035$ ,  $0.13$  and  $0.25 \text{ mmol/g}$  sorbed HDTMA revealed shapes and sizes of mordenite crystals (Fig. 5). The average crystal size was approximately  $1 \mu\text{m}$ . SEM observations confirmed the crystalline nature of mordenite and the crystal morphology which can be described in terms of closely bound aggregates of small platelets particles. These crystalline aggregates, however, were not clearly visible on the SEM micrographs of the MT samples with  $0.50$  and  $0.70 \text{ mmol HDTMA/g}$  due to surfactant coverage on the external crystal surface (Fig. 5).

### 3.8. Vibrational (FT infrared and FT Raman) spectroscopy

Vibrational bands of HDTMA in the range between  $3030$  and  $2800 \text{ cm}^{-1}$  in both, the IR and the Raman spectrum, were assigned to vibrational modes of methylene chains and trimethylammonium groups [36,37]. Weak infrared bands at  $3030$  and  $3017 \text{ cm}^{-1}$  were attributed to asymmetric and symmetric C–H stretching, respectively, of methyl in the surfactant head group (Fig. 6). A very weak band at  $3017 \text{ cm}^{-1}$  appeared in the spectra of the MT samples having HDTMA loadings of  $0.50$ ,  $0.70$  and  $0.85 \text{ mmol/g}$ , indicating higher concentration of the sorbed cations if compared to the FTIR spectra of the MT samples with lower HDTMA loadings ( $<0.25 \text{ mmol/g}$ ) where the respective vibrational band was not observed (Fig. 6).

Analogous to IR spectra, Raman bands at  $3030$  and  $3015 \text{ cm}^{-1}$  in the pure HDTMA spectrum were assigned to the asymmetric C–H stretching, and a weak band at  $2958 \text{ cm}^{-1}$  to the symmetric C–H stretching of the head methyl group (Fig. 7). Here again, a broad band at around  $3025 \text{ cm}^{-1}$  was observed only for the MT samples having initial HDTMA concentration higher than  $0.25 \text{ mmol/g}$  indicating higher amount of HDTMA cations sorbed on the zeolite (Fig. 7).

Asymmetrical and symmetrical  $\text{CH}_2$  stretching bands of hexadecyl chain are in general the most intense bands in the vibrational spectra of the pure HDTMA [38]. Position, width and height of these bands are extremely sensitive to the conformational changes of the chains. Narrow IR bands of the crystalline HDTMA at  $2918$  and  $2849 \text{ cm}^{-1}$  correspond to asymmetric and symmetric C–H stretching of the methylene groups, respectively, in *all-trans* alkyl chains. Introducing disorder into the chains, the bands become broader and they shift towards the high wavenumbers. The highest frequency shift ( $2929$  and  $2856 \text{ cm}^{-1}$ ) was observed in the spectrum of the MT sample with the lowest initial HDTMA amount ( $0.035 \text{ mmol/g}$ ) indicating that a significant number of sorbed HDTMA cation tails adopted *gauche* conformation (Fig. 6). On the other hand, variation in position of IR bands as much as  $1$  or  $2 \text{ cm}^{-1}$  was noted in the spectra of the MT samples having HDTMA loadings higher than  $0.25 \text{ mmol/g}$  implying an ordered structure of alkyl chains consisting of large number of *trans* conformers (Table 4 and Fig. 6).

Like the IR spectrum, the Raman spectrum of the crystalline HDTMA was dominated by the prominent bands of the methylene asymmetric and symmetric stretching modes at  $2880$  and  $2847 \text{ cm}^{-1}$ , respectively (Fig. 7) [39]. Although the frequency shifts of these bands in the spectra of the MT samples with sorbed HDTMA cations were not so dramatic, as it was the case in the IR spectra (Table 4), bands at around  $2885$  and  $2851 \text{ cm}^{-1}$  indicated higher portion of the *gauche* conformers in the MT samples with initial HDTMA concentration lower than  $0.25 \text{ mmol/g}$ . Bands at  $2882$  and  $2850 \text{ cm}^{-1}$ , on the other hand, which were noted in the spectra of the MT samples with initial HDTMA concentration higher than

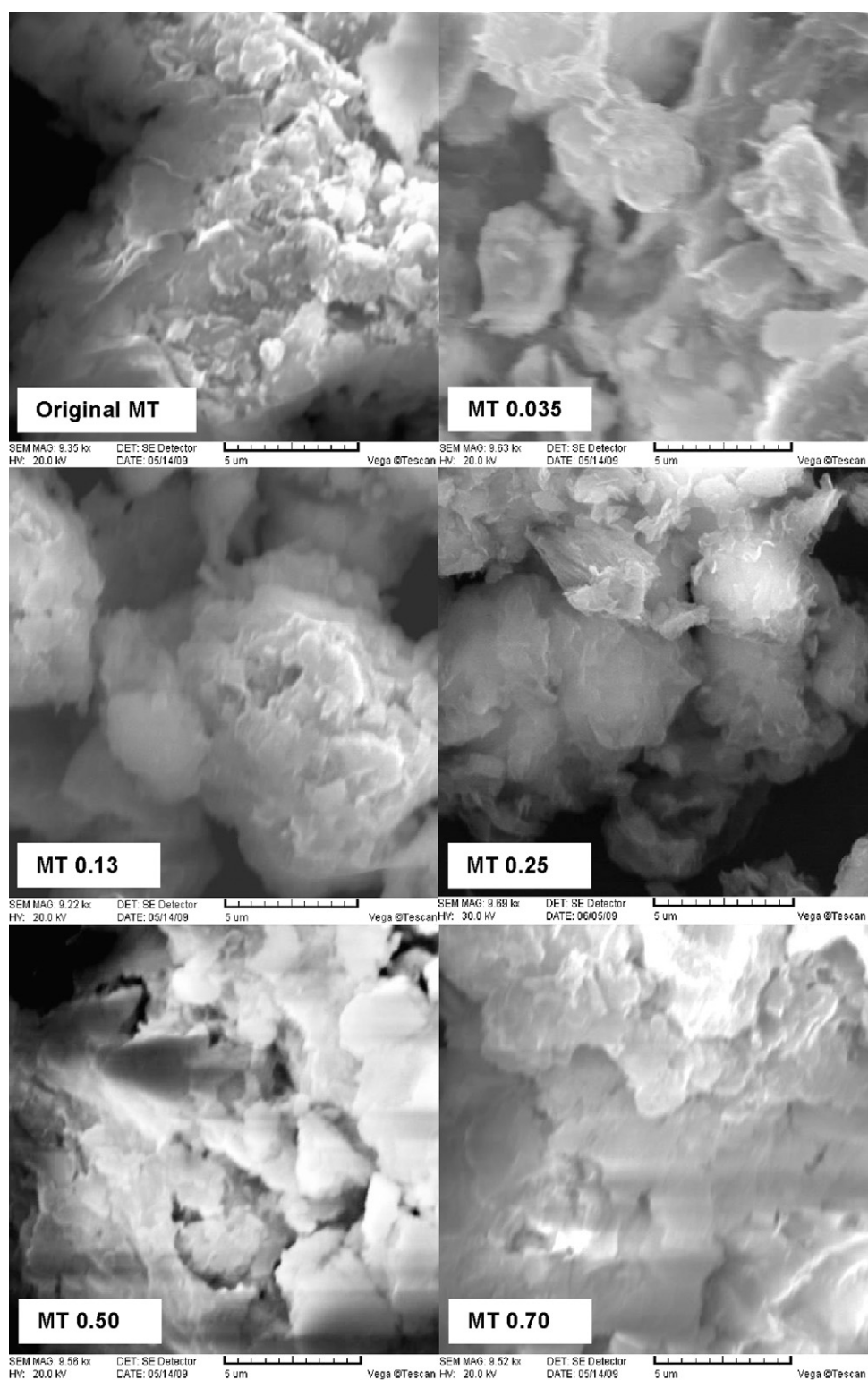


**Fig. 5.** Scanning electron micrographs of mordenite tuff (MT) samples. Labels MT 0.035–MT 0.70 denote initial amounts (mmol/g) of sorbed HDTMA cations.

0.25 mmol/g referred to the more ordered structure with higher number of *trans* conformers.

Conformation of alkyl chains strongly depends on concentration of the sorbed surfactant. In case of high concentration, the band positions resemble the ones of the pure HDTMA when chains adopt *all-trans* conformation. At low surfactant concentration, a conformational disorder occurs, resulting in higher number of *gauche* conformers. According to the vibrational mode wavenumbers it can

be concluded that the MT sample with the initial HDTMA amount of 0.035 mmol/g contained the lowest amount of sorbed HDTMA cations, followed by the MT samples with initial HDTMA loading in order of 0.13, 0.25, 0.70, 0.85 and 0.50 mmol/g. This was in agreement with the measured band intensities. The weakest IR absorption was observed for the MT sample with initial HDTMA amount of 0.035 mmol/g, and the strongest one for the MT sample with initial HDTMA amount of 0.50 mmol/g. Moreover, a sequence

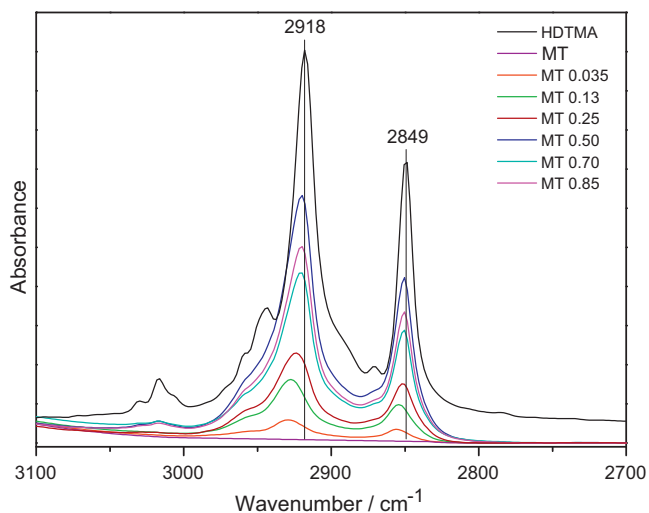


**Fig. 6.** FTIR spectra of the crystalline HDTMA, the original mordenite tuff (MT) and the modified MT samples in the C–H stretching region, 3100–2700  $\text{cm}^{-1}$ . Labels MT 0.035–MT 0.85 denote initial amounts (mmol/g) of sorbed HDTMA cations.

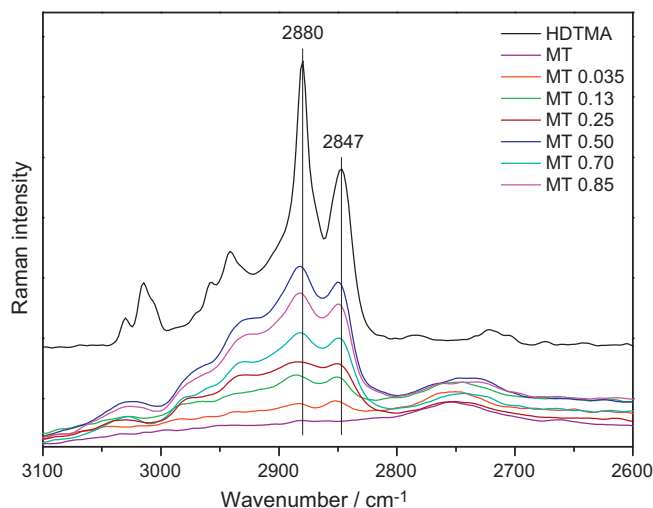


**Fig. 7.** FT Raman spectra of the crystalline HDTMA, the original mordenite tuff (MT) and the modified MT samples in the C–H stretching region, 3100–2700  $\text{cm}^{-1}$ . Labels MT 0.035–MT 0.85 denote initial amounts (mmol/g) of sorbed HDTMA cations.

of the Raman intensities concerning the C–H stretching modes matched the detected IR absorption values.

The ratio of the Raman intensities of the band at  $\sim 2880 \text{ cm}^{-1}$  to that at  $\sim 2850 \text{ cm}^{-1}$  ( $I_{2880}/I_{2850}$ ) is known to be sensitive to both the

**Table 4**

Position of the asymmetrical C–H stretching ( $\nu_{\text{as}}$  C–H) and symmetrical C–H stretching ( $\nu_{\text{s}}$  C–H) bands in the FTIR and FT Raman spectra of the crystalline HDTMA and the modified MT samples, and the Raman intensity ratio of the bands at  $\sim 2880 \text{ cm}^{-1}$  and  $\sim 2850 \text{ cm}^{-1}$  ( $I_{2880}/I_{2850}$ ). Labels MT 0.035–MT 0.85 denote initial amounts (mmol/g) of sorbed HDTMA cations.

Sample	FTIR		FT Raman		$I_{2880}/I_{2850}$
	Wavenumber/ $\text{cm}^{-1}$		Wavenumber/ $\text{cm}^{-1}$		
	$\nu_{\text{as}}$ C–H	$\nu_{\text{s}}$ C–H	$\nu_{\text{as}}$ C–H	$\nu_{\text{s}}$ C–H	
HDTMA	2918	2849	2880	2847	1.59
MT 0.035	2929	2856	2885	2852	0.98
MT 0.13	2927	2854	2885	2851	1.01
MT 0.25	2924	2852	2884	2851	1.01
MT 0.50	2920	2851	2882	2850	1.07
MT 0.70	2921	2851	2882	2850	1.03
MT 0.85	2920	2851	2882	2850	1.05

conformational disorder of the alkyl chains as well as to their packing [37]. For the crystalline HDTMA, the calculated ratio,  $I_{2880}/I_{2850}$ , was 1.59 whereas, for the HDTMA modified MT samples, it was around 1 (Table 4). Despite small variations in the calculated values regarding the treated MT samples,  $I_{2880}/I_{2850}$  of 1.07 suggested the most ordered structure in the MT with 0.50 mmol HDTMA/g, while the value of 0.98 confirmed the highest number of alkyl chain adopting *gauche* conformation in the MT with 0.035 mmol HDTMA/g.

#### 4. Conclusions

The natural mordenite tuff, consisting of only 30% of mordenite, sorbs higher amount of HDTMA cations than the clinoptilolite rich tuffs (50–80% of clinoptilolite) from our previous work [24]. This phenomenon could be due to large surface area of small mordenite crystals available for HDTMA cations sorption as well as diffusion of HDTMA into mesopores placed between mordenite platelets.

In mesopores HDTMA cations are placed parallel or tilted to the mordenite surface and individually separated, interaction among the alkyl chains is very weak resulting in formation of disordered *gauche* conformers. However, HDTMA sorption on the external surface, caused by an increase in concentration, leads to more efficient packing, strong interchain interaction and a high number of the ordered *trans* conformers. It is most likely that at the very high HDTMA loadings *trans* conformers form a bilayer ordering.

Different interactions of HDTMA cations with both, mordenite and clinoptilolite tuff (which have a different textural properties), might result in distinctive sorption abilities of these materials for the waste water treatment which will be the subject of our future research.

#### Acknowledgements

This work is done in the framework of the project No.125-1253008-3009: Membrane and adsorption processes for organics removal in water treatment, supported by the Croatian Education, Science and Sport.

#### References

- [1] D.W. Breck, Zeolite Molecular Sieves, Wiley, New York, 1984.
- [2] P. Kumar, P.D. Jadhav, S.S. Rayalu, S. Devotta, Surface-modified zeolite-A for sequestration of arsenic and chromium anions, *Curr. Sci.* 92 (2007) 512–517.
- [3] P. Castaldi, L. Santona, S. Enzo, P. Melis, Sorption processes and XRD analysis of a natural zeolite exchanged with  $\text{Pb}^{2+}$ ,  $\text{Cd}^{2+}$  and  $\text{Zn}^{2+}$  cations, *J. Hazard. Mater.* 156 (2008) 428–434.
- [4] B. Calvo, L. Canoira, F. Morante, J.M. Martínez-Bedia, C. Vinagre, J.-E. García-González, J. Elsen, R. Alcantara, Continuous elimination of  $\text{Pb}^{2+}$ ,  $\text{Cu}^{2+}$ ,  $\text{Zn}^{2+}$ ,  $\text{H}^+$  and  $\text{NH}_4^+$  from acidic waters by ionic exchange on natural zeolites, *J. Hazard. Mater.* 166 (2009) 619–627.
- [5] Z. Liang, J. Ni, Improving the ammonium ion uptake onto natural zeolite by using an integrated modification process, *J. Hazard. Mater.* 166 (2009) 52–60.
- [6] T. Motsi, N.A. Rowson, M.J.H. Simmons, Adsorption of heavy metals from acid mine drainage by natural zeolite, *Int. J. Miner. Process.* 92 (2009) 42–48.
- [7] M. Rožič, Š. Cerjan-Stefanović, L. Čurković, Evaluation of Croatian clinoptilolite- and montmorillonite-rich tuffs for ammonium removal, *Croat. Chem. Acta* 75 (2002) 255–269.
- [8] C.H. Ko, C. Fau, P.N. Chiang, M.K. Wang, LinF K.C., p-Nitrophenol, phenol and aniline sorption by organo-clays, *J. Hazard. Mater.* 149 (2007) 275–282.
- [9] Z. Rawafih, N. Nsour, Characteristics of phenol and chlorinated phenols sorption onto surfactant-modified bentonite, *J. Colloid Interface Sci.* 298 (2006) 39–49.
- [10] R. Zhu, L. Zhu, L. Xu, Sorption characteristics of CTMA–bentonite complexes as controlled by surfactant packing density, *Colloids Surf., A* 294 (2007) 221–227.
- [11] T.S. Anirudhan, M. Ramachandru, Surfactant-modified bentonite as adsorbent for the removal of humic acid from wastewaters, *Appl. Clay Sci.* 35 (2007) 276–281.
- [12] Z. Li, R.S. Bowman, Sorption of chromate and PCE by surfactant-modified clay minerals, *Environ. Eng. Sci.* 15 (1998) 237–244.
- [13] A. Patzko, J. Dekany, Ion exchange and molecular adsorption of a cationic surfactant on clay minerals, *Colloids Surf., A* 71 (1993) 299–307.

- [14] W. Rohl, W. von Rybinski, M.J. Schwuger, Adsorption of surfactants on low-charged layer silicates. Part I: Adsorption of cationic surfactants, *Prog. Colloid Polym. Sci.* 84 (1991) 206–214.
- [15] P.G. Slade, W.P. Gates, The ordering of HDTMA in the interlayers of vermiculite and the influence of solvents, *Clays Clay Miner.* 52 (2004) 204–211.
- [16] Z. Li, W.T. Jiang, H. Hong, An FTIR investigation of hexadecyltrimethylammonium intercalation into rectorite, *Spectrochim. Acta Part A* 71 (2008) 1525–1534.
- [17] T. Mehrian, A. de Keizer, A.J. Korteweg, J. Lyklema, Thermodynamics of adsorption of dodecylpyridinium chloride on Na-kaolinite, *Colloids Surf., A* 73 (1993) 133–143.
- [18] K. Hayakawa, T. Morita, M. Ariyoshi, T. Maeda, I. Satake, Adsorption of cationic surfactants on hydrophobic mordenites of different Si/Al ratio, *J. Colloid Interface Sci.* 177 (1996) 621–627.
- [19] B.K.G. Theng, Adsorption of alkylammonium cations by porous crystals, comparison between montmorillonite and synthetic near-faujasite, *N. Z. J. Sci.* 14 (1971) 1026–1039.
- [20] A.M. Yusof, N.A.N.N. Malek, Removal of Cr(VI) and As(V) from aqueous solutions by HDTMA-modified zeolite Y, *J. Hazard. Mater.* 162 (2009) 1019–1024.
- [21] Z. Li, Oxyanion sorption and surface anion exchange by surfactant-modified clay minerals, *J. Environ. Qual.* 28 (1999) 1457–1463.
- [22] E.J. Sullivan, D.B. Hunter, R.S. Bowman, Fourier transform Raman spectroscopy of sorbed HDTMA and the mechanism of chromate sorption to surfactant-modified clinoptilolite, *Environ. Sci. Technol.* 32 (1998) 1948–1955.
- [23] E.J. Sullivan, J.W. Carey, R.S. Bowman, Thermodynamics of cationic surfactant sorption onto natural clinoptilolite, *J. Colloid Interface Sci.* 206 (1998) 369–380.
- [24] M. Rožič, Đ. Ivanec Šipušić, L. Sekovanić, S. Miljanić, L. Čurković, J. Hrenović, Sorption phenomena of modification of clinoptilolite tuffs by surfactant cations, *J. Colloid Interface Sci.* 331 (2009) 295–301.
- [25] R.S. Bowman, E.J. Sullivan, Z. Li, Uptake of cations, anions, and nonpolar organic molecules by surfactant-modified clinoptilolite-rich tuff, in: C. Colella, F.A. Mumpton (Eds.), *Natural Zeolites for the Third Millennium*, De Frede Editore, Napoli, 2000, pp. 287–297.
- [26] J. Warchol, P. Misaelides, R. Petrus, D. Zamboulis, Preparation and application of organo-modified zeolitic material in the removal of chromates and iodides, *J. Hazard. Mater. B* 137 (2006) 1410–1416.
- [27] Z. Li, T. Burt, R.S. Bowman, Sorption of ionizable organic solutes by surfactant-modified zeolite, *Environ. Sci. Technol.* 34 (2000) 3756–3760.
- [28] H.K. Karapanagioti, D.A. Sabatini, R.S. Bowman, Partitioning of hydrophobic organic chemicals (HOC) into anionic and cationic surfactant-modified sorbents, *Water Res.* 39 (2005) 699–709.
- [29] P. Chutia, S. Kato, T. Kojima, S. Satokawa, Adsorption of As (V) on surface-modified natural zeolite, *J. Hazard. Mater.* 162 (2009) 204–211.
- [30] M. Majdan, S. Pikus, Z. Rzaczyńska, M. Iwak, O. Maryuk, R. Kwiatkowski, H. Skrzypek, Characteristics of chabazite modified by hexadecyltrimethylammonium bromide and of its affinity toward chromates, *J. Mol. Struct.* 791 (2006) 53–60.
- [31] M. Sprynskyy, T. Ligor, M. Lebedynets, B. Buszewski, Kinetic and equilibrium studies of phenol adsorption by natural and modified forms of the clinoptilolite, *J. Hazard. Mater.* 169 (2009) 847–854.
- [32] M. Rožič, Š. Cerjan-Stefanović, S. Kurajica, M. Rožmarić Mačefat, K. Margeta, A. Farkaš, Decationization and dealumination of clinoptilolite tuff and ammonium exchange on acid-modified tuff, *J. Colloid Interface Sci.* 284 (2005) 48–56.
- [33] G. Jozefaciuk, Effect of acid and alkali treatments on surface-charge properties of selected minerals, *Clays Clay Miner.* 50 (2002) 646–655.
- [34] E.J. Sullivan, D.B. Hunter, R.S. Bowman, Topological and thermal properties of surfactant-modified clinoptilolite studied by tapping-mode atomic force microscopy and high-resolution thermogravimetric analysis, *Clays Clay Miner.* 45 (1997) 42–53.
- [35] P. Sharma, P. Rajaram, R. Tomar, Synthesis and morphological studies of nanocrystalline MOR type zeolite material, *J. Colloid Interface Sci.* 325 (2008) 547–557.
- [36] Z. Li, W.-T. Jiang, H. Hong, An FTIR investigation of hexadecyltrimethylammonium intercalation into rectorite, *Spectrochim. Acta Part A* 71 (2008) 1525–1534.
- [37] N.V. Venkataraman, S. Vasudevan, Conformation of methylene chains in an intercalated bilayer, *J. Phys. Chem. B* 105 (2001) 1805–1812.
- [38] Y. Li, H. Ishida, Concentration dependent conformation of alkyl tail in the nanoconfined space: hexadecylamine in the silicate galleries, *Langmuir* 19 (2003) 2479–2484.
- [39] H. He, R.L. Frost, Y. Xi, J. Zhu, Raman spectroscopic study of organo-montmorillonites, *J. Raman Spectrosc.* 35 (2004) 316–323.